

# Response of atmospheric ground level temperatures to changes in the total solar irradiance

\*A. D. Erlykin <sup>1,2</sup>, and A. W. Wolfendale <sup>2</sup>

(1) P.N.Lebedev Physical Institute, Leninsky prosp., Moscow, Russia

(2) Department of Physics, Durham University, Durham, UK \*

June 17, 2015

## Abstract

The attribution of part of ‘global warming’ to changes in the total solar irradiance (TSI) is an important topic which is not, yet, fully understood. Here, we examine the TSI-induced temperature (T) changes on a variety of time scales, from one day to centuries and beyond, using a variety of assumptions. Also considered is the latitude variation of the T-TSI correlations, where it appears that over most of the globe there is a small increase in the sensitivity of temperature to TSI with time. It is found that the mean global sensitivity  $\alpha$  measured in  $K(Wm^{-2})^{-1}$  varies from about 0.003 for 1 day, via 0.05 for 11-years to  $\sim 0.2$  for decades to centuries. We conclude that mean global temperature changes related to TSI are not significant from 1975 onwards.

Before 1975, when anthropogenic gases were less important, many of the temperature changes can be attributed to TSI variations. Over much longer periods of time, Kyear to Myear, the TSI changes are more efficient still,  $\alpha$  increasing to about 0.5. Since 1975 the changes in mean global temperature are not due to TSI changes, but, rather to the increasing atmospheric  $CO_2$  content.

Keywords: total solar irradiance, surface temperature, sensitivity, correlations

## 1 Introduction

The role of changes in the Total Solar Irradiance (TSI) in the global warming debate is finite but uncertain; indeed, the latest IPCC Report (IPCC 2014a) quotes estimates for the radiative forcing from 1750 to the present of 0.0 to  $0.1 Wm^{-2}$  i.e. a very large range. It also refers to the fact that the value is model and time scale dependent. It is true that the TSI averaged over the Earth is approximately  $340 Wm^{-2}$  (as distinct from the value of  $\sim 1361 Wm^{-2}$  for incidence along the Sun-Earth direction) and the changes are only a fraction of one%, nevertheless, there are two main reasons for a detailed analysis, as follows.

---

\*corresponding author: tel.+74991358737, e-mail: erlykin@sci.lebedev. ru

- (i) Since the effect of global warming will be severe, it is imperative to understand every facet. The interaction of many factors affecting climate - with the attendant positive and negative feedback effects - can give rise to counter-intuitive correlations which need to be understood.
- (ii) An interesting aspect of the TSI variations concerns the apparent cloud cover, sunspot number (SSN) correlation, which some authors (e.g. Marsh and Svensmark 2000) have attributed to cosmic rays causing atmospheric nuclei, which in turn form cloud droplets, the intensity of which is well correlated with SSN. However, others, including ourselves (Erlykin et al. 2009) have presented evidence favouring TSI which is, of course, correlated with SSN. Since changes in cloud cover are intimately connected with climate change it is important to understand the effect of TSI changes.

We define the correlation (or, more strictly, the 'sensitivity') of (ground) temperature  $T$  with TSI as  $\alpha$ , in units of  $K(Wm^{-2})^{-1}$ ; linearity of changes of  $T$  with changes of TSI is assumed (see §2.1). The different values of  $\alpha$  by different workers have been considered by (IPCC 2014a; Erlykin and Wolfendale 2010; Lockwood 2007) and these works have not been analysed further. However, the values of  $\alpha$  are included in the final Figure for comparison. In the present work we make another examination and study latitude variations and temporal range effects, i.e. the extent to which induced temperatures depend on the length of time over which the increased radiation occurs. The former is because the latitude variation might help to explain the mechanism by which the changes in TSI are converted to temperature. The role of  $CO_2$  in climate change is examined and the year in which  $CO_2$  rather than TSI starts to dominate. In future, we will assume that ' $CO_2$ ' represents all anthropogenic gasses.

The changes caused by ENSO (ElNino Southern Oscillation) and PDO (Pacific Decadal Oscillation) are ignored because these are only partly Sun-induced ( obviously ) but consider their effect in §3.9. Similarly, we disregard volcanoes and aerosol effects at our level of accuracy. It is not impossible that the effects, other than TSI changes, contribute to the apparent TSI - Temperature correlation and in this case our  $\alpha$ -values represent upper limits. This aspect is considered later.

Inevitably, in this paper there will be some overlap with previous work. However, in view of the importance of the topic - and the new aspects - the work is considered to be justified.

## 2 Solar Variations

### 2.1 The basic data

We start by considering the basic data. Figure 1 gives the time series for TSI (TSI 2014) adopted by us. This relates to the total solar irradiance incident upon the Earth's atmosphere over all wavelengths. The errors, random and systematic, are not known but they are unlikely to be greater than  $0.07Wm^{-2}$  (i.e.  $\sim 0.5\%$  of the total, this being the average dispersion from year to year. We are mindful of problems of intercalibration

of satellite data (Zacharias 2014) but much of our analysis relates to data over 11-year intervals only. The dependencies of ‘temperature’ on time for two, important, latitude ranges are also shown (Zonal Temperatures 2014).

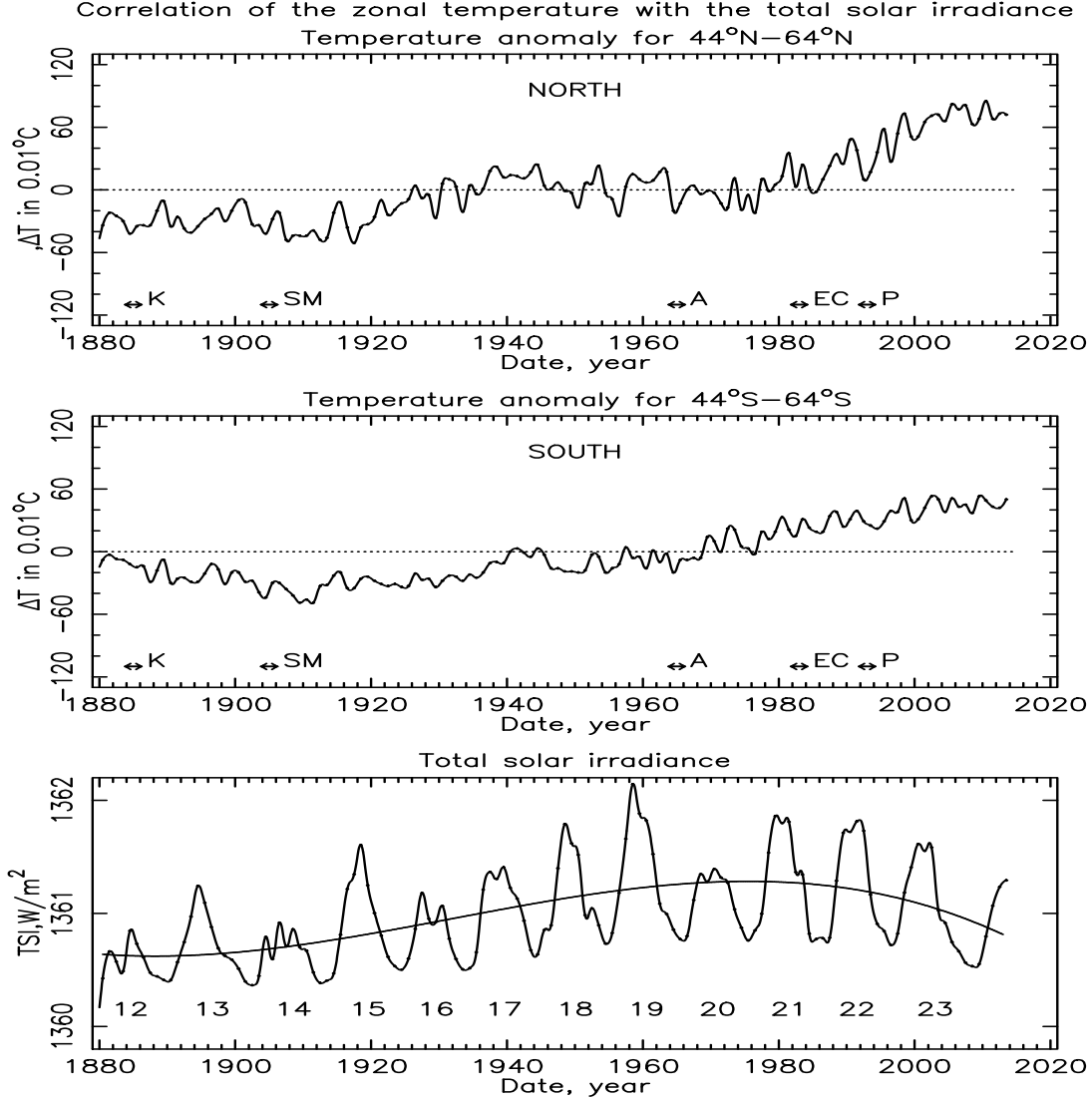


Figure 1: Basic data for the correlation of the zonal temperatures [5] with the total solar irradiance (TSI) [4] for the latitude ranges indicated. A smooth 3-degree polynomial fit has been made by us to the TSI data. The significant volcano time ranges are indicated. Key: K: Krakatoa; SM: Santa Maria; A: Aurang; EC: El Chichon; P: Pinatubo.

It will be noted immediately that the year by year dispersion of the temperature is much bigger in the North than in the South. After 1975 the temporal trends of the temperatures differ between North and South. This year (1975) is also where the TSI starts to fall.

Inspection of Figure 1 shows that for the Northern range  $\Delta T$  is increasing slowly with time. It means that part of the  $\alpha$ -values will arise from this cause. If the increase

in  $\Delta T$  were due to solar effects alone, the derived  $\alpha$ -value would be valid; however, if there is also another cause (the increase in  $\text{CO}_2$  density is significant) then it will be an upper limit.

The Southern results (Fig. 1, 1880-1975) are superior, in fact, because, as will be seen from Figure 1, the  $\Delta T$  values do not have an overall upward trend, they are the same in 1880 and 1975. Thus, the sensitivity derived from the data ( see Figure 2 ) should be reliable for the  $44^\circ - 64^\circ$  range.

## 2.2 The overall $\Delta T$ , TSI correlation from 1880

Figure 2 shows the dependence of  $\Delta T$  on TSI for data for each full hemisphere and for two periods: 1880-1975 and 1976-2013. The values of  $\alpha$  and correlation coefficient  $r$  are shown in the Figure.

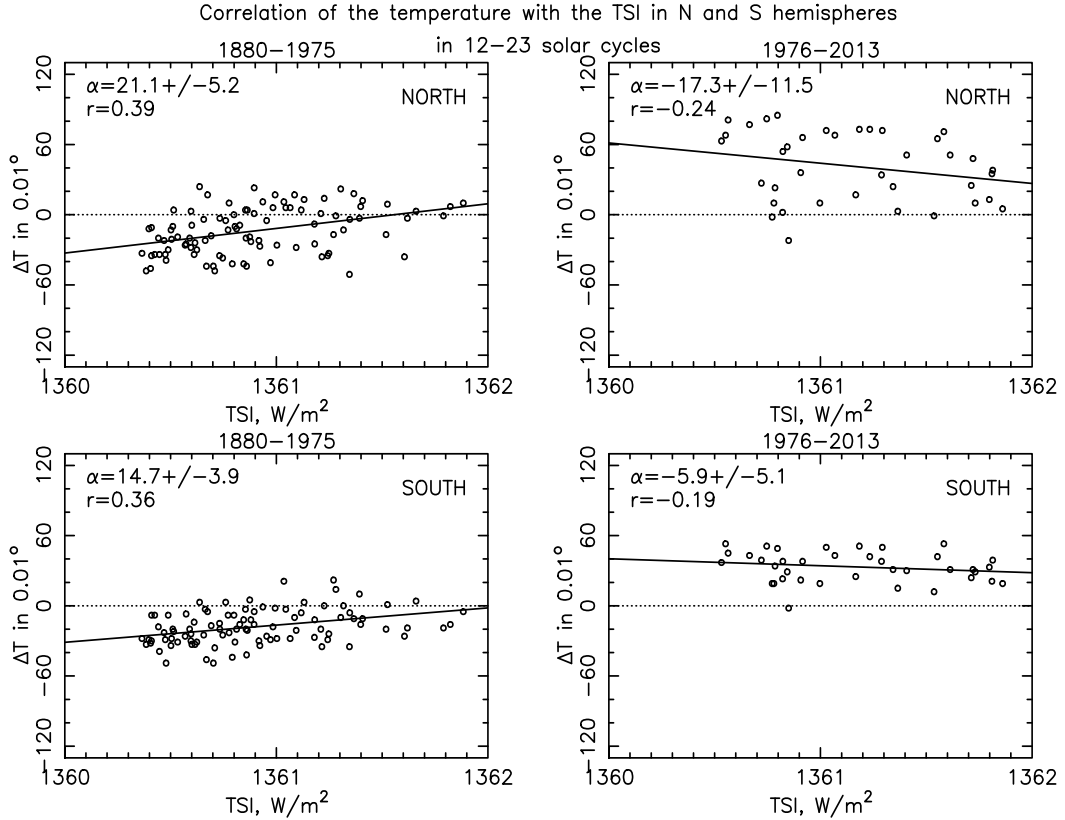


Figure 2: Correlation of the temperature anomaly  $\Delta T$  with the TSI for the two hemispheres and Solar Cycles 12-20 and 21-23 inclusive. The  $\alpha$ -values are given in the boxes.

Three features should be noted.

(i) It is evident that 1975 marked the transition. Positive  $\alpha$  values for 1880 - 1975 change sign and become negative after 1975. It means that after 1975 the temperature

anomaly  $\Delta T$  still goes up despite the fact that TSI goes down. This trend confirms the behaviour seen in Figure 1 for 44-64° latitude bands.

(ii) The sensitivity,  $\alpha$ , of  $\Delta T$  to TSI is higher in the Northern hemisphere than in the Southern hemisphere.

(iii) Fluctuations of  $\alpha$  measured for each solar cycle and latitude band, which are seen as a spread of points around the best fit line, are larger in the North than in the South.

All the above characteristics, pre-1975 - can be understood, in principle by the manner in which the 'ocean fraction' differs from one latitude band to another: the higher the ocean fraction, the higher the thermal inertia and consequent depression of the (short term) temperature variations.

## 2.3 Previous Decades

Although the accuracy of Mean global temperature estimates, and those of TSI are worse in the past than contemporary values, they are of value. Particularly useful are the plots of  $\Delta T$  and  $\Delta(TSI)$  versus time from (Lean 2004) which relate to 1600 to the present (from which we use 1600 - 1800). This range is complementary to our own studies of the period from 1900 to the present. Here, the sensitivity is  $\alpha = (0.24 \pm 0.05) K(Wm^{-2})^{-1}$ .  $\Delta T$  follows  $\Delta(TSI)$  faithfully, including the 'Little Ice Age' centered on about 1660, in apparent contradictions to the findings of (Foukal et al. 2012).

Another study has been made by (Scarfetta and West 2007, from which  $\alpha$  can be derived for two forms relating to the TSI. These give  $\alpha = 0.21$  and  $\alpha = 0.68$  in the usual units. The former, smaller, value of  $\Delta(TSI)$  over the Little Ice Age is from (Wang et al. 2005) and relates to data reported 5 years later. Thus, the value  $\alpha = 0.21$  is preferred. It should be remarked that these values do not suffer from the problem of  $\langle T \rangle$  changes due to  $CO_2$  increases.

# 3 The search for single solar cycle correlations and for longer periods

## 3.1 The latitudinal distribution of $\alpha$ for single Solar Cycles.

Figure 3 shows the  $\alpha$ -values versus Cycle No. for each latitude band. A number of features are worthy of note.

- i. There is a systematic increase of  $\alpha$  with time up to 1975 for most latitude bands (5 out of 8), which reverses after 1975.
- ii. There is no sign of an increased value of  $\alpha$  for near-equatorial latitudes, although absolute values of the temperature are the highest at the equator due to geometrical effects: the average solar intensity at Earth being clearly a diminishing function of latitude.
- iii. Inspection of the TSI as a function of time (Figure 1) shows that the TSI was highest for Cycle 19. Cycle 19 (Figure 4) shows a consistently high value of  $\alpha$ , at least for latitude ranges from 64 - 90N down to 24 - 44S.

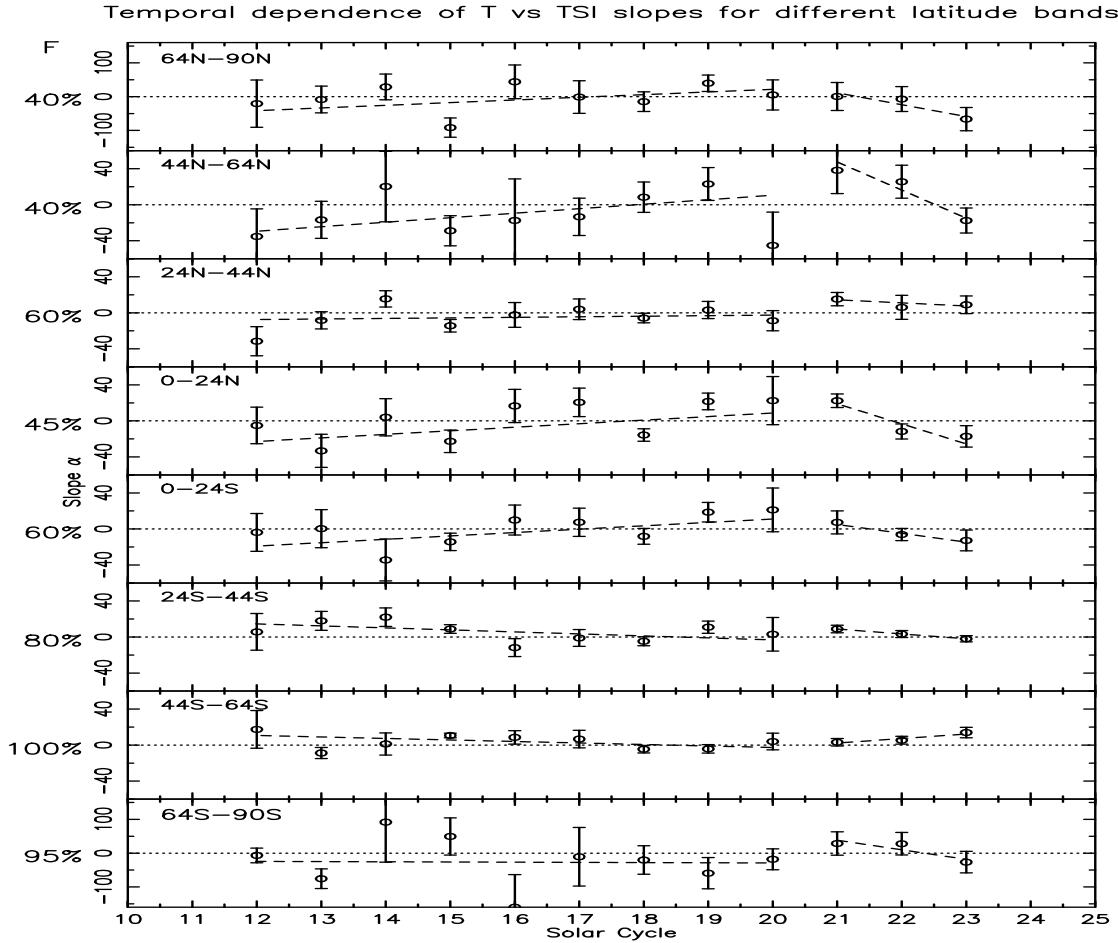


Figure 3: Values of  $\alpha$  versus Solar Cycle No for each latitude range. The straight lines are linear fits to the data both before and after Cycle 21. This Cycle is chosen because it is nearest to the peak of the TSI (see Fig.1) and also where the density of  $\text{CO}_2$  starts to increase significantly. Note that the vertical scale for polar regions 64N-90N and 64S-90S is different from the other latitude bands. F is the 'ocean fraction'.

- iv. There is a general agreement from latitude to latitude for each Cycle No, within the statistical errors where the best lines are taken as the 'datums'. Specifically, in terms of the individual errors, the differences from the best line are 38% (32%) above  $1\sigma$  and 5% (5%) above  $2\sigma$ , where  $\sigma$  is the standard deviation and the values in brackets are the percentages expected for a Gaussian distribution of errors.

An important point is that the results suggest that variations within limited regions of the Earth (latitude bands) - particularly in the Northern Hemisphere - are representative of the whole Earth. For example, large European areas can be so representative. Inspection of the Solar Cycles which experienced major volcanoes (Figure 1) in Figure 5, show virtually no difference from the other Cycles.

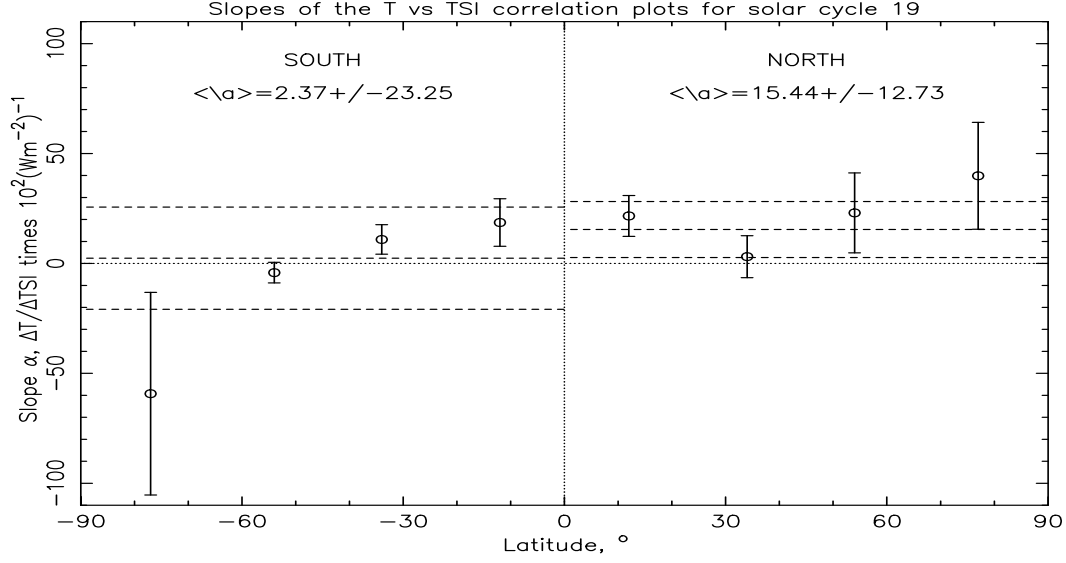


Figure 4:  $\alpha$ -values for Solar Cycle No.19. The vertical lines represent the means and associated one standard deviation errors. The overall mean value is  $0.06 \pm 0.13$ .

### 3.2 The hemispheric variation of $\alpha$ for single Solar Cycles

We have averaged the values of  $\alpha$  for single Solar Cycles shown in Figure 3 separately for Northern and Southern hemispheres. Figure 5 shows the results. The dispersion of the values of  $\alpha$  about their mean is clearly much greater for the North than for the South.

The mean values of  $\alpha$ , which includes the stated errors, give the values indicated in the Figure. There is an indication of the slow rise of the sensitivity of northern T to TSI with time ( $\alpha = (2.29 \pm 1.99) \cdot 10^{-2} \text{ K(Wm}^{-2})^{-1}$  per cycle, which reverses after 1975 ( $\alpha = -(14.3 \pm 11.5) \cdot 10^{-2}$  per cycle in the same units), starting from the 21st Solar Cycle. Again this feature is better seen in the North than in the South, where  $\alpha$  has no time variability.

### 3.3 An alternative method for determining $\alpha$

Instead of the TSI, a related quality, the Sun-spot number (SSN) has been adopted: the two are not quite exactly proportional. The results are shown in Figure 6. The corresponding value of  $\alpha$  is:  $\langle \alpha \rangle = (0.06 \pm 0.03) \text{ K(Wm}^{-2})^{-1}$  as described in the caption.

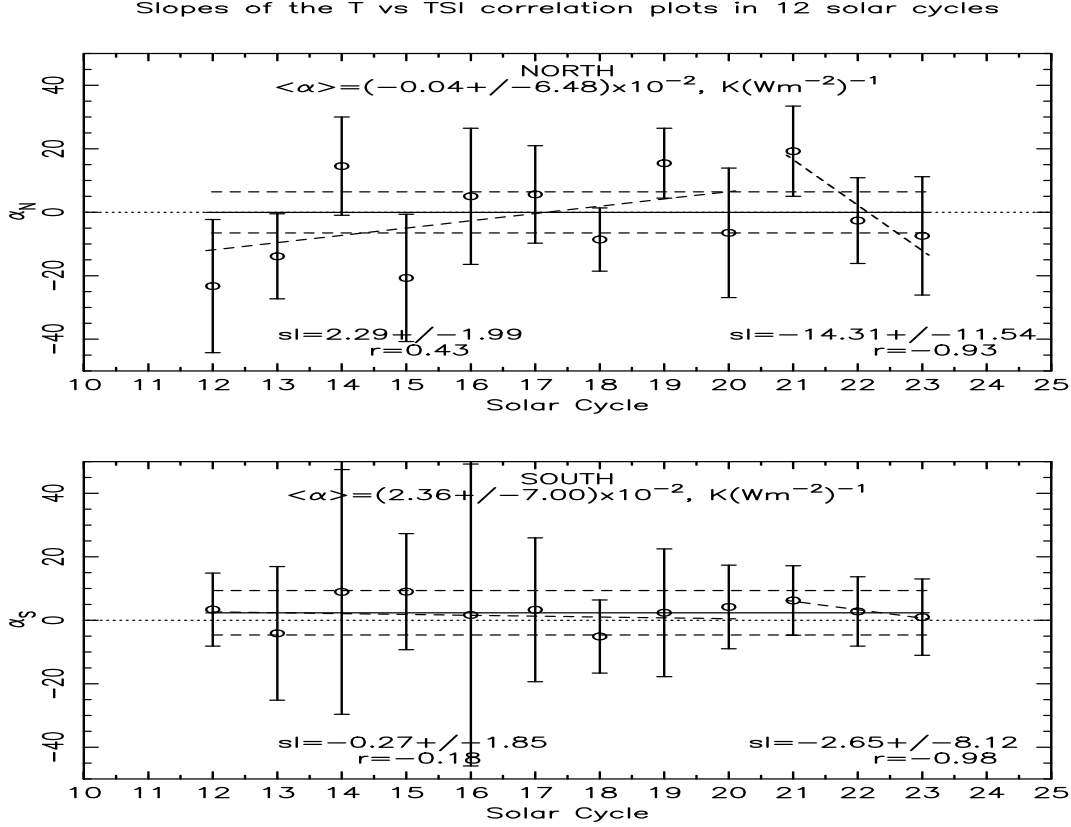


Figure 5: The sensitivity ( $\alpha$ ) of the  $\Delta T$  vs TSI correlation plots for North and South and for each Solar Cycle, 12-23 inclusive.  $\alpha$  is measured in units of  $K(Wm^{-2})^{-1}$ . The means and their one standard deviation errors are indicated.

### 3.4 Differences in $\alpha$ correlated with the fraction of the Earth's surface covered by water

Returning to Figure 3, we draw attention to the straight lines drawn through the  $\alpha$ -values, separately, for Solar Cycles 12-20 and 21-23. The border of 1975 is chosen because this is where the temperature starts to increase rapidly in most latitude bands and where anthropogenic gases start to increase significantly.

The possible role of seas/oceans can be considered. Figure 7 shows the temporal speed of rise for  $\alpha$ , viz.  $d\alpha/dN$ , where  $N$  is the solar cycle number, versus fraction of the latitude band covered by water, the 'ocean fraction,  $F$ '. The statistically significant linear trend of  $d\alpha/dN$  with  $F$  for Cycles 12-20 shows that  $d\alpha/dN$  for any ocean fraction,  $F$ , can be found by weighting it by linear interpolation of a high value for  $F=0$  and a low value for  $F=100\%$ . This result clearly arises because of the great thermal inertia of the oceans.

The inversion in  $d\alpha/dN$  for cycles 21-23, i.e. where the temperature is increasing rapidly, implies that another mechanism is involved. A likely cause is, as remarked



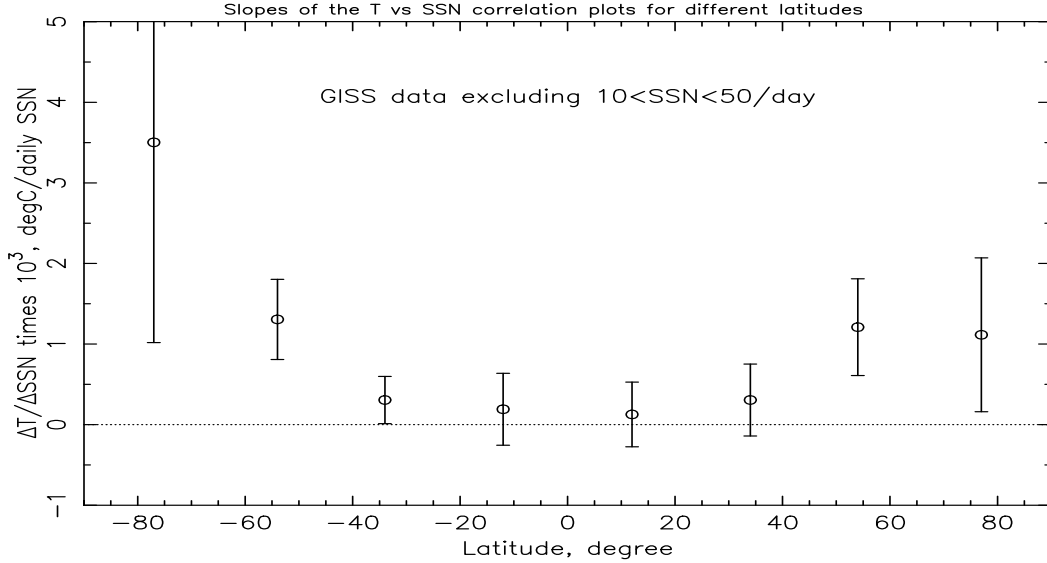


Figure 6: Slopes of  $\Delta T$  versus Sunspot numbers (SSN) for each latitude range. On this scale, unity corresponds to  $\alpha = 0.15^\circ\text{K}(\text{Wm}^{-2})^{-1}$ . The overall mean,  $0.48 \pm 0.24$ , corresponds to  $\langle \alpha \rangle = 0.072 \pm 0.036 \text{K}(\text{Wm}^{-2})^{-1}$ .

earlier, the anthropogenic gases which start to rise rapidly at about 1960 (Etheridge et al. 1996) and thus their delayed effect will start somewhat later.

We have also searched for a correlation of temperature as such with the ocean fraction, with the results shown in Figure 8. It is seen that the higher ocean fraction corresponds to the decrease of the temperature rise observed in 1880-1975. It is another piece of evidence showing the importance of the higher thermal inertia of the ocean compared with that of the land.

### 3.5 Time delays caused by thermal inertia

It is obvious that thermal inertia will cause a delay in response to a change in energy input (TSI) as well as a reduction in the magnitude of  $\alpha$ . The average TSI has an apparent minimum about 1890, which might be expected to manifest itself in a minimum in the ensuing temperature change. Using temperature plots for the various latitude ranges from (TSI 2014) we have determined the year of the first minimum (e.g. 1920 for 44-64S, where there is nearly 100% ocean). A plot of delay versus ocean percentage yields a straight line at the 3.7 sigma level (2% probability). For 100% ocean the delay is about 30 years. Similar results appear for other features of the temperature series (Figure 9). Clearly, such long delays are responsible for the reduced values of  $\alpha$  for solar cycles, but less so for intervals of several decades. Returning to Figure 7, if a linear extrapolation of the fit to the lowest ocean fraction is allowed, the value of  $\alpha$  is  $0.075 \text{ K}(\text{Wm}^{-2})^{-1}$  over land alone.

Temporal behaviour of T vs TSI sensitivity as a function of the ocean fraction

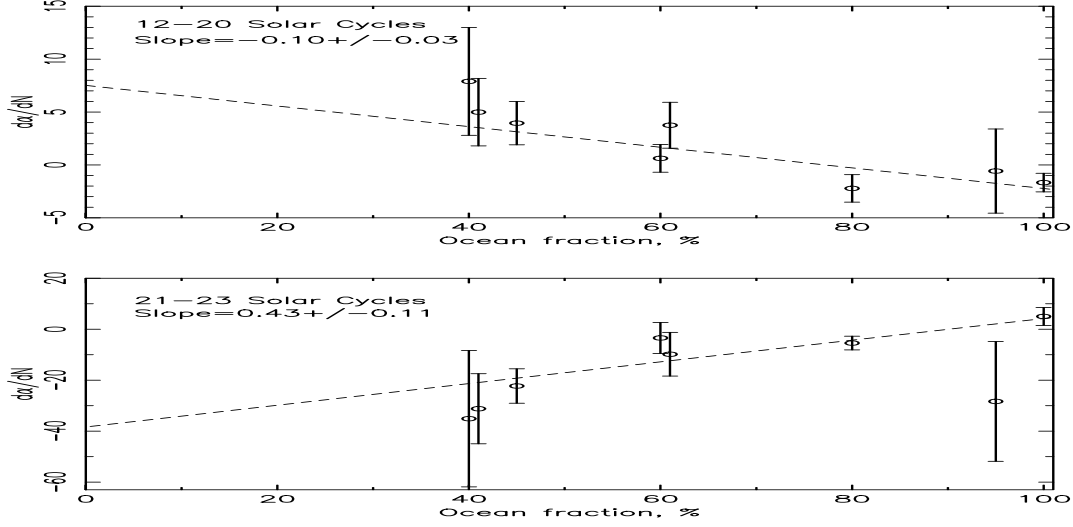


Figure 7: Variation of  $d\alpha/dN$ , where N is the Solar Cycle number, as a function of the ocean fraction: upper panel is for Cycles 12-20, lower panel is for Cycles 21-23.

### 3.6 Relevance of $CO_2$ to latitudinal variations

We continue by considering the source of the  $CO_2$  density observations. The dependence of the global mean  $CO_2$  density as a function of time is from (IPCC 2014b). Recent values are, in ppm, for the year in brackets: 315(1960), 323(1970), 335(1980), 352(1992), 366(2000) and 385(2010). There is very little difference between the N- and S-hemispheres but there are small latitude variations such that the highest  $CO_2$  densities are for  $35^\circ N$  and  $32^\circ S$ , for July, 2008.

There is seen to be some correlation with the results of Figure 2, i.e. the slopes of  $\alpha$  vs SSN, for  $24^\circ-44^\circ N$  and  $24^\circ-44^\circ S$  are slightly smaller than the overall average, beyond Solar Cycle 20.

On a longer time scale, it can be noted that there is apparent evidence for a direct connection between  $\alpha$  and the TSI itself, independently of any  $CO_2$  effects. This shows itself as a temporal correspondence (1975) between the maximum value of  $\alpha$  (Figure 10) and that of the TSI (Figure 1).

Explanations will be advanced later.

Following the remarks in the previous sections about anthropogenic gases (referred to here as ' $CO_2$ '), we give, in Figure 10, a plot of  $\alpha$  as such against  $CO_2$  content with respect to a datum of 240ppm (IPCC 2014b).

### 3.7 The average value of $\alpha$ for time ranges of several decades

Figure 2 gives an average (for N and S) over nearly 95 years of  $(17 \pm 3) \cdot 10^{-2} K(Wm^{-2})^{-1}$  and in the text (§2.2). For a longer period, some 350y, we have  $(21 \pm 5) \cdot 10^{-2} K(Wm^{-2})^{-1}$ . Both are shown in Figure 11 and both are seen to be similar to other

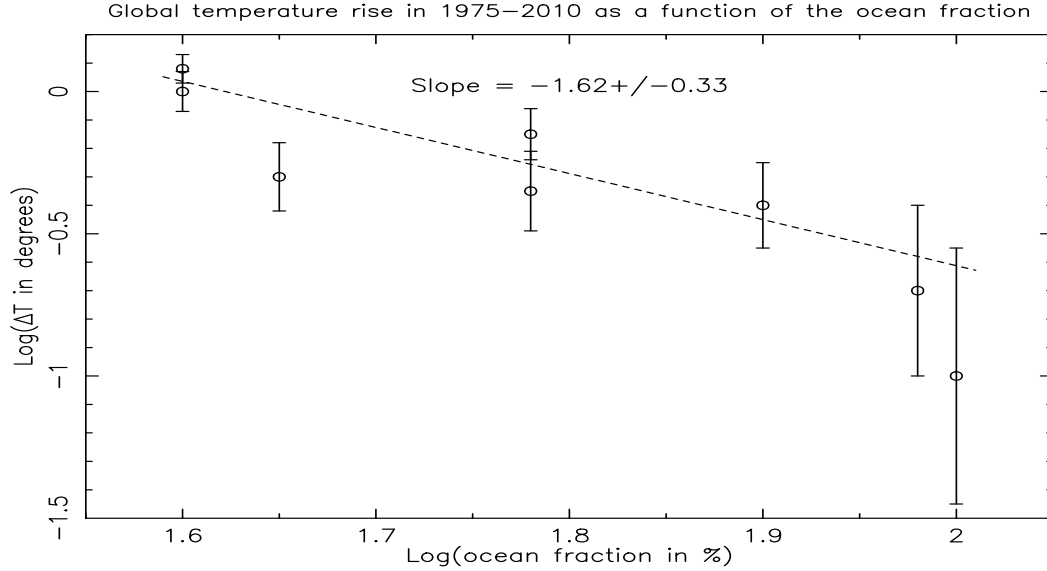


Figure 8: Temperature changes from 1975 to 2010,  $\Delta T$  for each latitude band as a function of the ocean fraction,  $F$ . Note that we plot  $\log \Delta T$  against  $\log F$ .

estimates (by us, Erlykin and Wolfendale 2010).

### 3.8 An estimate of $\alpha$ for the last 6000 years

Inevitably, measurements of Temperature and TSI over historic time (thousands of years) are inaccurate, being derived from proxies. However, tentative estimates have been made (Mann et al. 1998) from which an approximate value of  $\alpha$  can be derived. No doubt other parameters affect the global temperature besides TSI but there is a tolerable correlation of  $\Delta T$  and (proxy) sunspot number for the last 6000 years. The approximate value of  $\alpha$  is  $0.29 \text{ K}(Wm^{-2})^{-1}$ .

### 3.9 The effect of ENSO and PDO on $\alpha$

In the Introduction it was pointed out that ENSO and PDO were ignored, i.e. their effect on the derivation of  $\alpha$  was not included. It is of interest, however, to see to what extent  $\alpha$  is dependent on ENSO and PDO, and other parameters, too, specifically the number of sunspots at maximum, the 'width' of the cycle ( i.e. minimum to minimum ) and the aa magnetic index. In each case  $\alpha$  is plotted against the parameter in question and a straight line fitted. The slopes of these lines in terms of their standard deviation from the mean are given in Table 1 for both the North and South hemispheres.

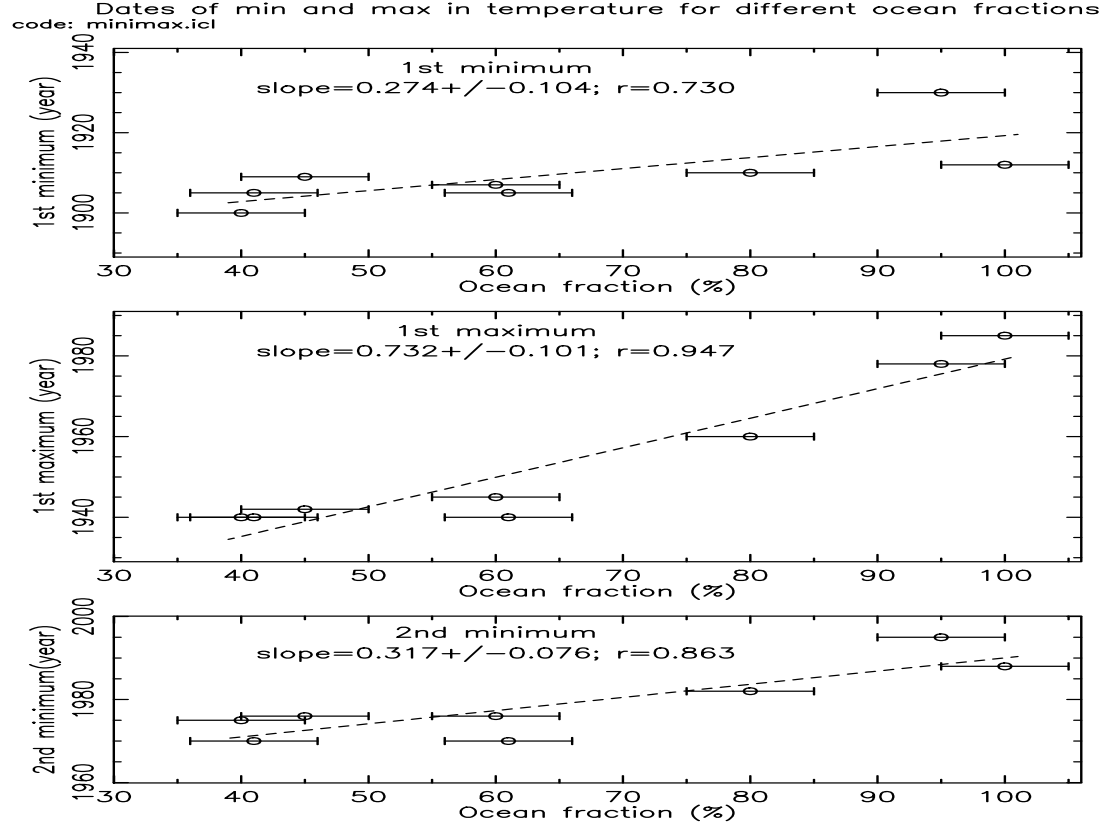


Figure 9: Year of the minimum and maximum in temperature profile for different ocean fractions.

Parameter	North	South
PDO	2.6	0.7
ENSO	0.3	2.0
Max.SSN	1.4	2.0
Cycle Width	4.4	5.2
aa magnetic index	4.4	0.2

Table 1. Slopes of  $\alpha$  versus parameter in terms of their number of standard deviations from zero

It will be noted that the only (statistically) significant correlations are with cycle width and the aa magnetic index, both indicators directly related to the Sun.

## 4 Discussion of the Results

### 4.1 The validity of the $\alpha$ -values and their explanation

There is evidence for a finite but very small value of  $\alpha$  for Solar Cycles, as such. An average estimate from the results presented is  $\langle \alpha \rangle = (0.07 \pm 0.02) K(Wm^{-2})$ , averaged

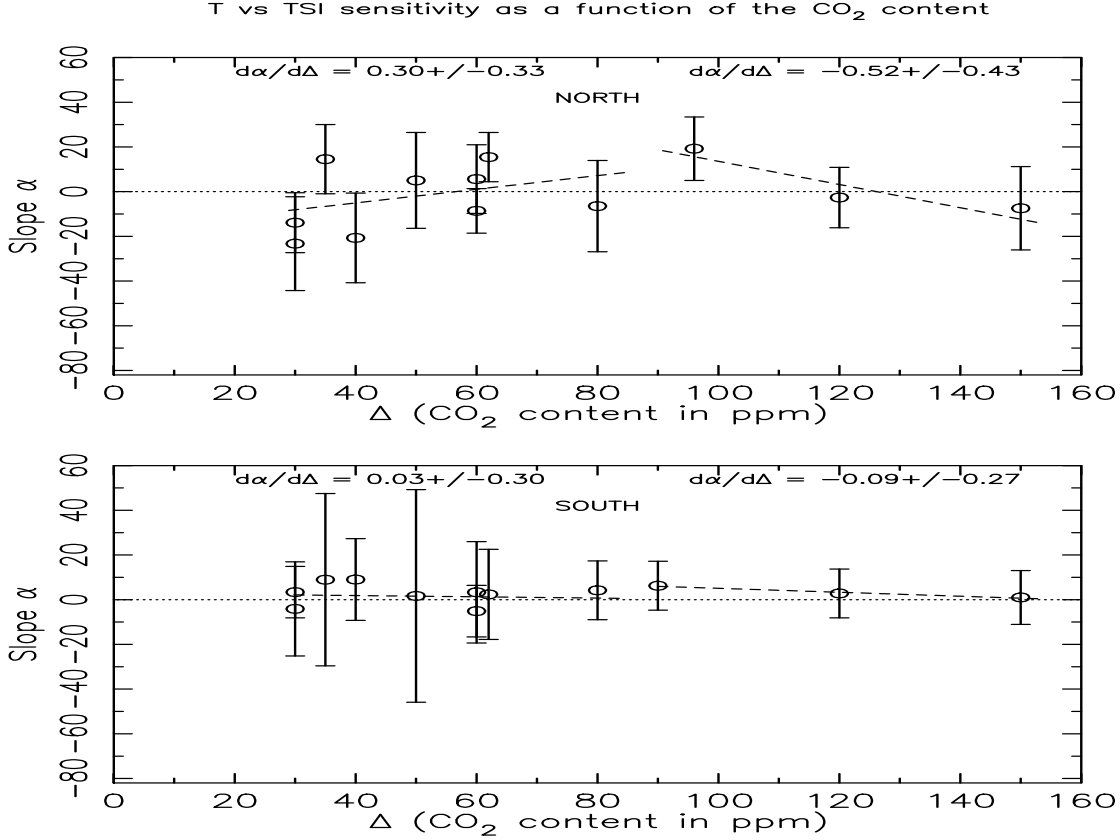


Figure 10: Temporal behaviour of  $\alpha$  as a function of  $\text{CO}_2$  content, the  $\text{CO}_2$  datum being 240ppm. 90ppm corresponds approximately to the situation for 1975. It is evident that there must be additional sources of error in the North for  $\Delta \leq 100$

from 1890 using the values from Figures 4, 6 and 7. This is indicated in Figure 11, where it is compared with the results of other workers: it is seen to be in the region where there is rough consistency between the results of others.

There seems little latitudinal variation of the values of  $\alpha$  apart from the clear correlation with ocean fraction (see Figure 7) and the small effect mentioned in §3.6. The increasing diminution with time after Cycle 20, which is a prominent feature in Figure 3, is attributed, by us, to the effect of anthropogenic gases, as remarked already, but, in fact the correlation in Figure 10 needs further study (see §4.3).

## 4.2 The time dependence of $\alpha$

Figure 7 represents an apparently new feature of the interrelation of the rate of change of  $\alpha$  with ocean fraction and some discussion is necessary.

Firstly, the value of  $\Delta\alpha/\Delta N \sim 0$  for 100% ocean fraction in both cases (TSI rising and TSI falling) is interesting, in that it shows that this situation ('all ocean') leads to a near temporal stability of  $\alpha$ .

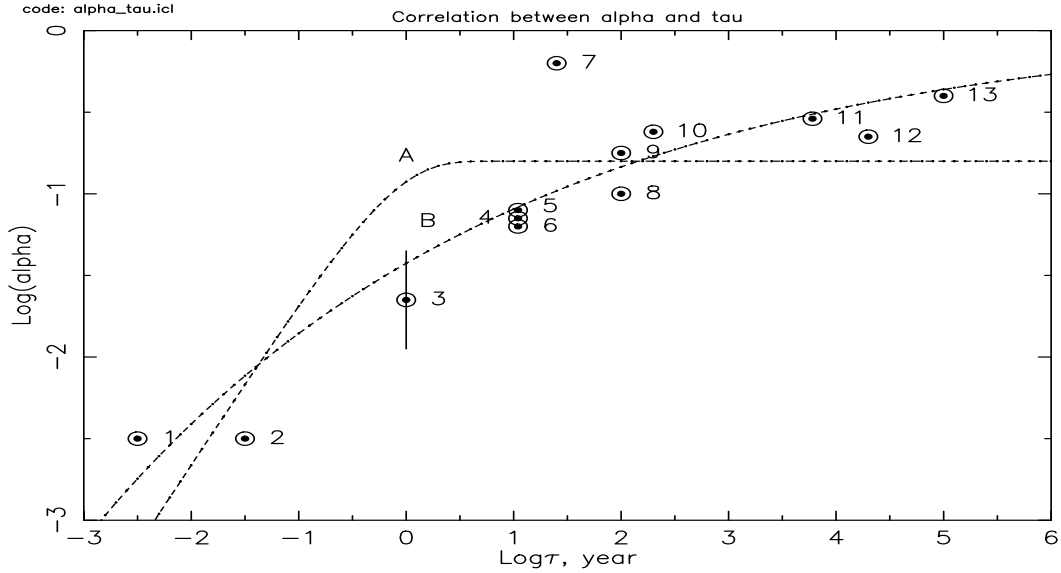


Figure 11:  $\alpha$ -values, i.e. sensitivity of mean global temperature to Total Solar Irradiance, over various time intervals  $\tau$ ,  $\alpha$  is measured in  $K(Wm^{-2})^{-1}$ . Key: see separate sheet. Note the logarithmic scales.

The difference in the slopes before and after 1975 indicates that, for the ‘mainly land’ region,  $\Delta\alpha/\Delta N$  is more sensitive to TSI changes after 1975 than before. It is perhaps the effect of TSI on the  $CO_2$  which is largely responsible for the ‘greenhouse effect’ or simply the reduction in  $\alpha$  for the 11-year cycle caused by the fact that there is no (appreciable) 11-year cyclical variation in the  $CO_2$  density, i.e. the temperature goes up but TSI cyclical changes have a diminishing effect. The latter explanation is preferred.

The extrapolation for ‘all-land’ is seen to be high - as would have been expected, and may be relevant for large land areas with comparatively stable climates.

### 4.3 The latitude dependence of $\alpha$

It was mentioned at the start that there might be additional information, related to climate change, from analysis of the latitude variation of various parameters.

That this is the case can be seen from Figures 4, 6 and 7. The ‘latitude-effect’ appears to be well-explained by the dependence of the ocean-fraction on latitude, the increased thermal inertia of the oceans having a damping effect which reduces  $\alpha$ . The damping period can be seen in Figure 9.

The important role of 1975 as the year when the ‘greenhouse effect’ due largely to  $CO_2$  started to dominate the temperature rise (Figure 8.)

An interesting further fact can be seen in Figure 3, where for Cycles 21, 22 and 23, the slopes vary with latitude in a particular way. Figure 8 gives an explanation in terms of oceanic fractions. Inspection of IPCC Report (IPCC 2014b) reveals estimates of the likely temperature rises as a function of latitude and longitude, for the period 2016

to 2036,  $CO_2$  being largely responsible for the temperature increases. Their latitude dependence mirrors that of the negative slope of  $\alpha$  versus Solar Cycle No,  $N$ , as can be seen in Table 2. Thus, the higher the efficiency of T-change due to  $CO_2$ , ( $\Delta T(CO_2)$ ), the greater the (negative) slope of  $\delta\alpha/\delta N$ .

Latitude Range (deg.)	$\delta\alpha/\delta N$	$\Delta T(CO_2)$
$>64^\circ N$	1.2	2.0
$44-64^\circ N$	1.0	1.4
$24-44^\circ N$	0.35	0.9
$0-24^\circ N$	0.8	0.9
$0-24^\circ S$	0.45	0.5
$24-44^\circ S$	0.25	-0.1
$44-64^\circ S$	-0.25	0
$>64^\circ S$	0.8	0.7

Table 2. Latitude variation of the variation of  $\alpha$  with Solar Cycle No. ( $\delta\alpha/\delta N$ ), in arbitrary units, (from Figure 3) and the predicted change in temperature from 2016 to 2036 ( $\Delta T(CO_2)$ ), in deg. K (IPCC 2014b)

The fit is at the 5 sigma level and the probability (of non-correlation) is 0.5%.

The fraction of the ‘recent’ temperature rise due to changes in the TSI is an important parameter that needs discussion. If we consider 1900 as the starting point and 1975 as a recent datum, the appropriate value of  $\alpha$  to use is  $0.2K(Wm^{-2})^{-1}$  (Figure 11). The increase in temperature expected for  $\Delta(TSI)$  of  $0.6Wm^{-2}$  is thus  $0.12^\circ K$ . This can be compared with the measured increase of  $0.4^\circ K$  (TSI 2014), i.e. 30%. This is, clearly, not a negligible fraction.

Since 1975 the TSI has fallen by  $0.46(Wm^{-2})^{-1}$  and our expected temperature reduction is  $0.10^\circ K$ . In this time the mean global temperature rise has been  $0.50^\circ K$  thus the TSI change gives a reduction of 20%. Without the TSI change, the temperature rise would have been  $0.6^\circ K$ . The  $0.10^\circ K$  difference is not negligible and may contribute to the apparent fall in rate of rise in temperature after 1975 (the well-known ‘hiatus’).

## 5 Comparison with the results of other workers and conclusions

The results are compared in Figure 11. The values for 1 day and 1 year are simplistic determinations, by us, for day/night temperature differences and seasonal differences, respectively. There is a general consensus of the values of  $\alpha$ .

Considering the 11-year solar cycle, it is interesting to note that those determinations which studied the individual components of temperature change: TSI, ENSO, volcanoes and a general rise (Lockwood 2007; Lean 2004; Haigh 2007) denoted 5 and 6, reached the same ‘solar value’ as our mean: (4) in Figure 11. This is not to say that ENSO et al. have no effect on climate but their effects come partly from TSI. This is also true to some extent for  $CO_2$  changes which are, in part, caused by increased ocean temperatures.

The global values of  $\alpha$  are collected together in Figure 9 and details are given in Table 2. Smooth lines through the points illustrate the effect of the thermal inertia of the globe. The lines need an explanation. That marked A is the standard form for, for example, the charging of a condenser through a resistor:  $\alpha = \alpha_0(1 - \exp(-\frac{\tau}{\tau_0}))$  where  $\tau_0$  is the effective time constant. That marked B is for the standard form but for  $\log\alpha$  versus  $\log\tau$  and is thus more of an empirical fit.

A possible explanation is that we have the sum of two (weighted) curves of type A, one for land and one for oceans, the values of  $\tau_0$  being different. In first approximation  $\tau_0 \simeq 1$  year for land and  $\simeq 30$  years for ocean.

To conclude, we have demonstrated that solar effects become increasingly important until about 1975, following which another mechanism (anthropogenic gases?) take over. Understandably, the role of the oceans, and their considerable thermal inertia, is important.

There is consistency between the results from different authors and a smooth plot of sensitivity of atmospheric temperature versus change in TSI seems appropriate from days to hundreds of thousands of years.

- All the factors considered by us confirm the conclusion by climatologists that TSI changes dominated as the cause of increasing global temperatures before about 1975 but that another cause (presumably anthropogenic gases) is responsible for the ‘rapidly’ increasing temperatures in the most recent 40 years.

### **Acknowledgements**

The authors are grateful to the Kohn Foundation for financial support and to Professor Terry Sloan for helpful comments.



## 6 Table 3. Key to the points in Figure 11

Slopes ( $\alpha$ -values) from various sources versus the 'integration time' to which the values relate ( $\tau$ ). Typical errors are  $\pm$  a factor 2.

1. Daily variation. Present work. 1d.
2. Forbush decreases.  $\sim 10$  d. (Laken 2012)
3. Summer/Winter vs. latitude. 1 year. (Erlykin and Wolfendale 2010)
4. Solar Cycle. Present work: §4.1. 11 years
5. Solar Cycle. 11 years (Lockwood 2007, Lean et al. 2005)
6. Solar Cycle. 11 years (Haigh 2007)
7. 'Long dip'. 25 years (Erlykin and Wolfendale 2010)
8. Maunder minimum. 100 years (Lean et al. 2005)
9. Previous decades. Present work: §4.2. 100 years
10. Ditto. 200 years
11. Long-term. Present work: §2.4. 6000 years
12. Last Ice Age.  $2 \cdot 10^4$  years (Haigh 2007)
13. Orbital changes.  $10^5$  years. Rusov V. et al., 2008, private communication (si-iis@t.e.net.ua)

### References

Erlykin AD, Gyalai G, Kudela K, Sloan T, Wolfendale AW, 2009, Some aspects of ionization and the cloud cover, cosmic ray correlation problem, *J. Atmos. and Solar-Terr. Physics*, 71, 823-829; doi:10.1016/j.jastp.2009.03.007

Erlykin AD, Wolfendale AW, 2010, Global cloud cover and the Earth's mean surface temperature, *J. Atmos. and Solar-Terr. Physics*, 31/4, 399-408; doi:10.1007/s10712-010-9098-7(10pp)

Etheridge DM, Steele LP, Langenfelds RL, Francey RJ, Barnola JM, Morgan I, 1996, Natural and anthropogenic changes in atmospheric  $CO_2$  over the last 1000 years from air in Antarctic ice and firn, *J. Geophys. Res.*, 101, 4115-4128

Foukal P, 2012, A new look at solar irradiance variation, *Solar Physics*, 279, 365-381; doi:10.1007/s11207-012-0017-6(17pp)

Haigh J.D., 2007, The Sun and the Earth's climate, *Living Rev. Solar Phys.*, 4, 2

IPCC Report, 2014a, Climate change, the physical science basis, ch 8 Anthropogenic and natural radiation forcing, 659-740

IPCC Report, 2014b, Climate change, the physical science basis, ch 11 Near-time climate change projections and probability, 959-1029

Laken B , Wolfendale AW, Kniveton D, 2012, Cosmic ray decreases and changes in the liquid water fraction over the oceans, Geophys. Res. Lett., L23803(5pp)

Lean JL., 2004, Solar irradiance reconstruction, IGBP pages/World Data Centre for Paleoclimatology, Data contribution series #2004-035, NOAA/NGDC Paleoclimatology Program, Boulder, Co, USA (29pp)

Lean JL, Rottman G, Harder J, Kopp G, 2005, SORCE contribution to new understanding to global change and solar variability, Solar Phys., 230, 27-53

Lockwood M, 2007, Recent changes in solar outputs and the global mean solar temperature. III Analysis of contributions to global mean air surface temperature rise. Proc. Roy. Soc. A, doi:10.1098/rspa.2007.0348

Mann ME, Bradley RS, Hughes MK, 1998, Global-scale temperature patterns and climate forcing over the past six centuries, Nature, 392, 779-787

Marsh ND, Svensmark H, 2000, Low cloud properties influenced by cosmic rays, Phys. Rev. Lett., 85, 5004-7

Scafetta N, West B.J., 2007, Phenomenological reconstructions of the solar signature in the Northern Hemisphere surface temperature records since 1660, J. Geophys. Res., 112, D24503 (10pp)

TSI 2014, [http : //lasp.colorado.edu/data/sorce/tsi\\_data](http://lasp.colorado.edu/data/sorce/tsi_data)

Wang Y-M, Lean JL, Speeley NR, 2005, Modeling the Sun's magnetic field and irradiance since 1713, Astrophys. J., 625, 522-538

Zacharias P, 2014, An independent review of existing total solar irradiance, Surveys in Geophys., 35, 897-912

Zonal temperatures: [http : //data.giss.nasa.gov/gistemp/tabledata\\_v3](http://data.giss.nasa.gov/gistemp/tabledata_v3)